Available online at www.sciencedirect.com
ScienceDirect
Applied Catalysis B: Environmental 78 (2008) 176–182
APPLIED CATALYSIS B: ENVIRONMENTAL
www.elsevier.com/locate/apcatb

Influence of amine template on the photoactivity of TiO_2 nanoparticles obtained by hydrothermal treatment

G. Colón [a,*], M.C. Hidalgo [a], J.A. Navío [a], E. Pulido Melián [b], O. González Díaz [b], J.M. Doña [b]

[a] *Instituto de Ciencia de Materiales de Sevilla, Centro Mixto CSIC-Universidad de Sevilla, Américo Vespucio s/n, 41092 Sevilla, Spain*
[b] *Centro Instrumental Químico-Físico para el Desarrollo de Investigación Aplicada (CIDIA), Departamento de Química, Universidad de Las Palmas de Gran Canaria, Edificio Central del Parque Científico Tecnológico, Campus de Tafira, 35017 Las Palmas, Spain*

Received 19 June 2007; received in revised form 22 August 2007; accepted 15 September 2007
Available online 20 September 2007

Abstract

TiO_2 nanoparticles have been prepared by amine template-assisted sol–gel precipitation and further hydrothermal treatment. We have investigated the effect of different amines (hydrazine and triethylamine) in the final surface and structural properties. It has been stated that the different amounts of amine could act as an interesting template upon hydrothermal treatment. Further thermal treatment also leads to a significant improvement in the photocatalytic properties of the studied systems. Surface and morphological features notably differ from TiO_2 prepared using different synthetic routes. Wide surface and structural characterization of the samples have been carried out, and correlations with precipitation pH are pointed out from this characterization. In all cases, amine template TiO_2 obtained exhibit high conversion values for phenol photo-oxidation reaction. Further calcination treatment of all the studied systems clearly leads to photocatalytic conversions higher than that exhibited by TiO_2 Degussa P25.

Keywords: TiO_2; Hydrazine; Triethylamine; Alkoxide; Sol–gel; Hydrothermal; Photocatalysis

1. Introduction

Titanium dioxide is one of the most important photocatalyst and many works have been devoted to the preparation and modification of this semiconductor [1,2]. It is well established that morphological and structural parameters strongly affect the photocatalytic activity of a semiconductor [2]. From the point of view of the enhancement in the efficiencies of the photocatalytic process, it is evident that the tailoring and development of new and alternative photocatalysts can be considered of great interest. The development of new photocatalytic system goes through the modification in the synthetic process as well as the design of new systems and configurations (nanotubes, mesoporous, thin films, etc.) [2]. With regard to TiO_2, these modifications would involve, among other approaches, the generation of nanosized particles [3].

The synthesis of nanoparticles with controlled size and composition is of technological interest. As a consequence, there has been a lot of highlighting on the production of nanoparticulated TiO_2 for a wide range of applications, including photocatalysis. Within this framework, the proposal of new synthetic routes for obtaining highly active nanoparticulated TiO_2 appears extremely interesting. In this sense, Wang et al. reported that there is an optimal particle size for photo-oxidation of chloroform on nanocrystalline TiO_2 [4,5]. For an intrinsic TiO_2 they found it to be around 10 nm. This optimum was attributed to the optimum in surface reaction versus e^-/h^+ recombination.

Therefore, the improvement of the final photocatalytic properties might be achieved by influencing those properties, which control either the charge carrier dynamics (carrier generation, transfer and diffusion) or the surface catalytic process, which are the quality of the structure and the surface features. In this sense, it is widely reported that the hydrothermal synthesis would provide the adequate structural and surface properties for photocatalytic applications [6]. The

* Corresponding author.
E-mail address: gcolon@icmse.csic.es (G. Colón).

0926-3373/$ – see front matter © 2007 Elsevier B.V. All rights reserved.
doi:10.1016/j.apcatb.2007.09.019

occurrence of the appropriate features, affected by controlling the preparation steps, significantly influences the photo and catalytic parts of the photo-oxidation mechanism [6,7]. It is assumed that for a good photocatalytic activity a slow recombination of the excess charge carriers and an efficient charge transfer from surface to the reactants are necessary [8,9]. Those premises are directly affected by the semiconductor structure [9]. That means that a good candidate might have not only the adequate surface area and porosity but also a high structural quality, which implies the lack of impurities, defects or amorphous domains resulting from the synthetic route or reagents.

Takahashi et al. described an interesting method for obtaining Ti^{4+} aqueous solution by means of amine complexation [10]. Moreover, some authors have recently reported the use of organic modifiers such as amines in the preparation of TiO_2 by hydrothermal route [11,12]. The addition of these templating organic species allows the control of the final morphology and hence their properties [13]. In this sense, in a previous paper we reported a wide study of highly photoactive TiO_2 systems prepared by hydrothermal method from a Ti^{4+} water solution [14]. The correlations between the route parameters and the final surface and structural properties demonstrate the importance of controlling the synthetic steps. The best photocatalyst in that series presented well-crystallized anatase structure with low crystallite size (ca. 10 nm), with high surface area values and the cleanest surface situation after hydrothermal treatment. Though the surface area contribution for this system is not the only property controlling the high photoactivity, the structural features could not compete with Degussa P25. And thus, the best photocatalyst in our series do not reach the specific rate exhibited by the commercial Degussa one. We concluded, that the structural features affecting to the electronic transfer and diffusion of charge carriers might be improved in order to compete with Degussa photocatalyst.

For this purpose we continue with the study of hydrothermally treated TiO_2 from Ti^{4+} water solution. In the present case, we study the effect of using different amine precipitating agent (hydrazine and triethylamine) as well as the effect of post-calcination treatment.

2. Experimental

Different TiO_2 series have been obtained by precipitation of initial aqueous Ti^{4+} stock solutions using different amines and further hydrothermal treatment. These precursor solutions were obtained by adding certain amount of Ti^{4+}-isopropanol solution (38.4 ml of TTiP + 38.2 ml of isopropanol) to 400 ml of distilled water at pH 2 achieved by means of acetic acid. After TTiP addition a white precipitate is obtained that upon stirring at room temperature for 1 week evolve to a milky homogeneous solution. A certain amount of hydrazine (HYD) or triethylamine (TEA) was then added drop wise to the Ti-solution aliquot till the desired pH value (8 and 11).

The obtained white precipitate suspension (150 ml, which corresponds to 75% of the total reactor volume) was then placed in a Teflon recipient inside of stainless steel autoclave. The hydrothermal treatment was performed at 120 °C, 24 h. At the same time, the calcined set of samples was obtained by further calcination of the hydrothermally treated powders. The influence of this thermal treatment was studied at 300 and 500 °C for 3 h.

BET surface area measurements were carried out by N_2 adsorption at 77 K using a Micromeritics 2000 instrument. Pore volumes were determined using the cumulative adsorption of nitrogen by the BJH method.

X-ray diffraction (XRD) patterns were obtained using a Siemens D-501 diffractometer with Ni filter and graphite monochromator. The X-ray source was Cu Kα radiation. We have calculated the mean crystallite size (D) from the line broadening of corresponding X-ray diffraction peaks, according to Scherrer equation (peaks were fitted by using a Voigt function):

$$D = \frac{\lambda \times 180}{\pi \cos\theta L}$$

where L is the line width at medium height, λ the wavelength of the X-ray radiation 0.15406 nm and θ is the diffracting angle.

Diffuse reflectance spectra were obtained on a UV–vis scanning spectrophotometer Shimadzu AV2101, equipped with an integrating sphere, using $BaSO_4$ as reference. UV–vis spectra were performed in the diffuse reflectance mode (R) and transformed to a magnitude proportional to the extinction coefficient (K) through the Kubelka–Munk function, $F(R_\infty)$. Band gap values were obtained from the plot of the modified Kubelka–Munk function $(F(R_\infty)E)^{1/2}$ versus the energy of the absorbed light E [15].

Samples were also studied by transmission electron microscopy (TEM) using a Philips CM200 instrument. The microscope was equipped with a top-entry holder and ion pumping system, operating at an accelerating voltage of 200 kV and giving a nominal structural resolution of 0.21 nm. Samples were prepared by dipping a 3 mm holey carbon grid into ultrasonic dispersion of the oxide powder in ethanol.

Photocatalytic runs (2 h) of phenol oxidation over the different catalysts (1 g/l) were performed in a Pyrex immersion well reactor (450 ml) using a medium pressure 400 W Hg lamp supplied by Applied Photophysics, showing main emission line at 365 nm. In the oxidation tests, an oxygen flow was used to produce a homogenous suspension of the catalyst in the solution. Before each photo-experiment, the catalysts were settled in suspension with the reagent mixture for 15 min in the dark. The evolution of the initial phenol concentration (ca. 50 ppm in water) was followed by UV–vis spectrometry through the evolution of its characteristic 270 nm band, using a filtered aliquot ca. 2 ml of the suspension (Millipore Millex25 0.45 μm membrane filter). In all cases, after 120 min irradiation the 100% conversion is reached, and then the degradation rates were calculated from the slopes of the conversion plots at the first 15 min of reaction, and assuming a zero-order kinetics at this stage of the reaction.

Table 1
Surface and structural characterization for TiO_2 samples

Sample	120 °C, 24 h			300 °C, 3 h			500 °C, 3 h		
	S_{BET} (m^2/g)	Band gap (eV)	Crystallite size (nm)	S_{BET} (m^2/g)	Band gap (eV)	Crystallite size (nm)	S_{BET} (m^2/g)	Band gap (eV)	Crystallite size (nm)
HYD pH 8	161	3.4	10	109	3.3	12	68	3.3	18
HYD pH 11	183	3.7	9	135	3.3	12	74	3.3	17
TEA pH 8	172	3.3	10	99	3.3	13	59	3.3	18
TEA pH 11	140	3.3	12	97	3.4	13	63	3.3	18

3. Results and discussion

3.1. Hydrothermal treated samples

In our previous study [14], we reported the influence of the starting Ti^{4+} water solution as well as the effect of precipitation pH in the final properties of hydrothermally obtained TiO_2. The best route was that in which Ti stock solution was prepared by using acetic acid and further precipitation with TEA at higher pH values. After the hydrothermal treatment, anatase phase and high surface area values were obtained (115–130 m^2/g). In Table 1 we summarize the surface and structural characterization data for the set of samples studied in the present paper. The specific surface area values obtained by precipitation with hydrazine and TEA at different pH values ranged between 140 and 183 m^2/g. The precipitation at pH 8 with hydrazine and TEA leads to similar surface area TiO_2 (160–170 m^2/g). However, the precipitation at higher pH value produces a different evolution in both cases. Thus, meanwhile for hydrazine the higher pH slightly increases the surface area, for TEA the contrary effect is observed. Subsequently, at pH 8, TiO_2 exhibit similar surface areas whereas at pH 11 surface areas appear significantly different (183 m^2/g vs. 140 m^2/g).

In Fig. 1 we show the evolution of pore distribution for samples prepared by hydrothermal method. For samples prepared by precipitation with hydrazine the average pore diameter indicates a certain influence with the pH value. Thus, at pH 11, the average pore diameters slightly shift to lower values (from 128 to 110 Å), which correspond to an increase in surface area. For samples precipitated with TEA no differences are found in the pore size distribution, and in both samples at different pH values the average pore diameter is around 75 Å, in spite of the diminution in the S_{BET} value. Nevertheless, it is worthy to note that comparing both set of systems, the highest pore diameters would correspond to hydrazine-precipitated TiO_2.

Regarding to the structural features of hydrothermal systems, in all cases, anatase phase is the only present. No influence in the type of amine is observed regarding to the structural pattern of TiO_2. The crystallite sizes reported in Table 1 indicate similar values for all systems (9–12 nm). In any case, the small differences observed at pH 11 are in agreement with the surface area evolution above described.

TEM images of selected samples (Fig. 2) denote a great homogeneity in shape and size in the hydrothermally obtained system particles. It is worthy to note no significant aggregation in the particles. In all cases, small roundish particles of around 10 nm are observed. This observation is in accordance with the crystallite size values obtained from XRD data.

The UV–vis diffuse reflectance spectra (not shown) are also in good agreement with the structural features described above. All systems show similar absorption spectra with absorption edges around 400 nm and the band gap values calculated from these plots are around 3.3 eV for TEA precipitated systems and 3.4–3.7 eV for hydrazine ones (Table 1). So, as we previously reported, though some authors described the incorporation of nitrogen by precipitation using ammonia or other amine systems [16,17], this behaviour is not observed in our systems, which do not exhibit any absorption in the visible range. Thus, amine only would act as precipitating agent by complexing in certain way to Ti^{4+} precursor [14] and probably affecting to the surface and structural properties of final system [18].

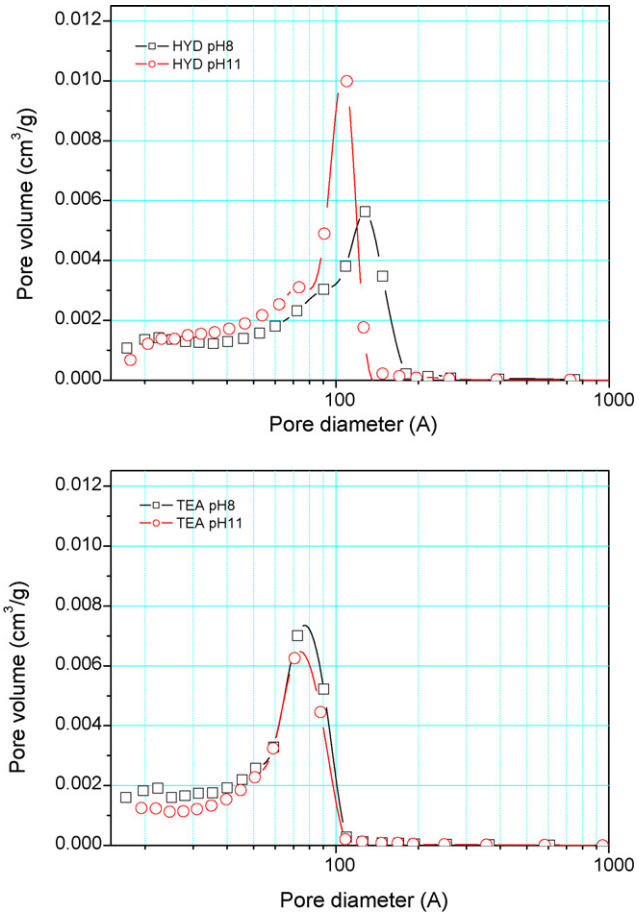

Fig. 1. Pore size distribution of hydrothermally obtained systems.

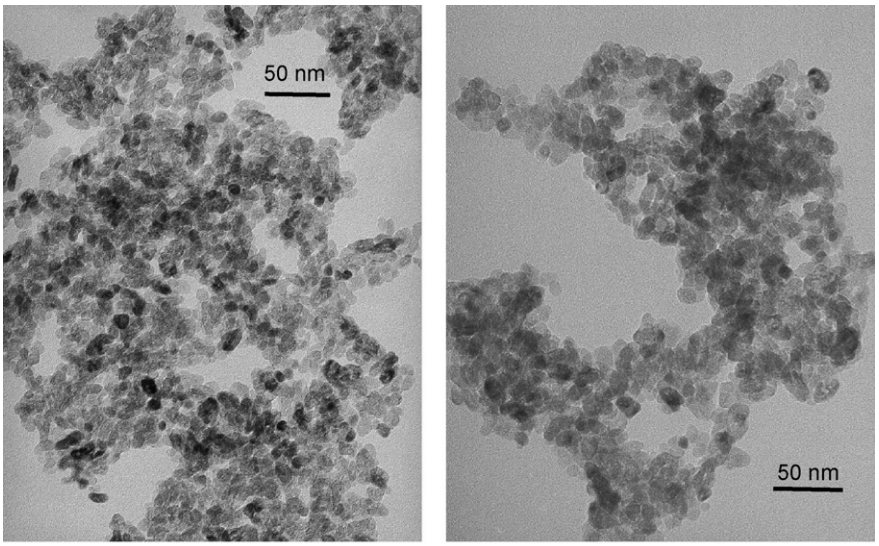

Fig. 2. TEM images of selected samples: (a) TiO_2 TEA at pH 8 and (b) TiO_2 TEA at pH 11.

In Fig. 3 we represent the photocatalytic behaviour of hydrothermally treated samples precipitated using TEA and hydrazine at different pH values. The reaction rate values for HYD systems appear slightly lower than Degussa P25 one (Fig. 3a). On the contrary, TEA series present reaction rates slightly higher than Degussa one. Moreover, for these systems it seems that as pH increases reaction rates trend somewhat to increase while for hydrazine precipitated one, the reaction rate appear to be similar. From these results, the best photoactivity is achieved for TiO_2 precipitated with TEA at pH 11. By the analysis of the specific reaction rates per surface area unit (Fig. 3b), all systems appear with a significantly lower conversion rates with respect to Degussa P25. This fact clearly indicates an important surface area factor in the photocatalytic activity of these hydrothermally prepared TiO_2. Thus, though their conversion rates per gram of catalyst showed similar values as commercial Degussa, it is evident that the high surface area values exhibited by our samples directly affects the photoactivity. If we compare the photoactivity behaviour of the prepared TiO_2, it seems that the differences observed in S_{BET} values for systems precipitated at pH 11 (183 m^2/g vs. 140 m^2/g for hydrazine and TEA, respectively), do lead to an important difference in the conversion rates. Thus, it might be inferred that a certain improvement in the crystallinity of TiO_2 prepared from TEA would balance this different surface contribution, enhancing the photoactivity in the case of the sample precipitated with TEA at pH 11.

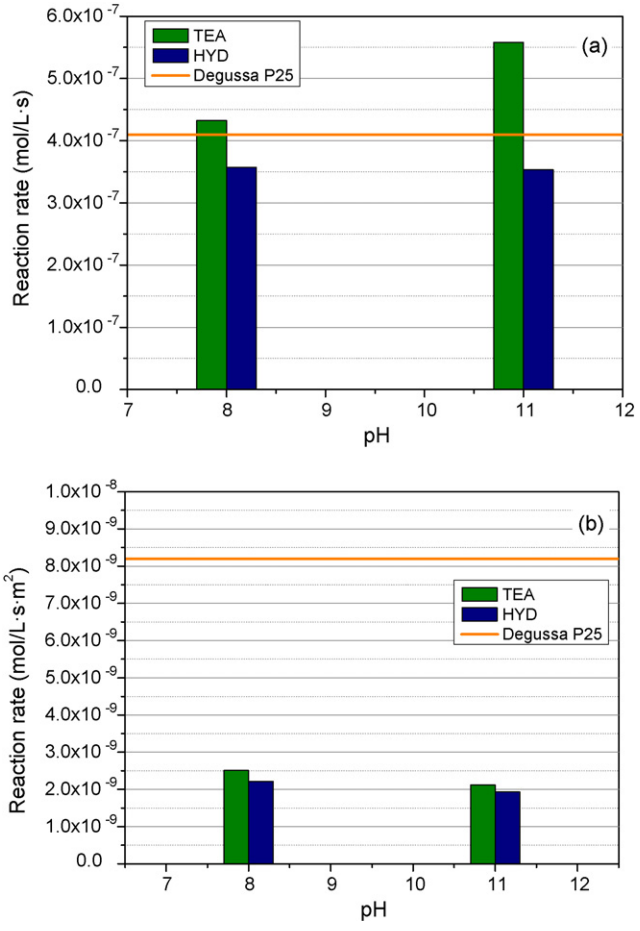

Fig. 3. (a) Photocatalytic activity of hydrothermally obtained systems and (b) photocatalytic activity per surface area unit of hydrothermally obtained systems.

3.2. Post-calcined samples

It is clear that the hydrothermal treatment leads to improved surface area TiO_2 photocatalysts exhibiting for this reason similar conversion rates than Degussa P25. In order to enhance the structural features we have studied the effect of a post-calcination treatment over the hydrothermally obtained TiO_2 systems.

In Table 1 we report the surface area values for hydrothermally treated and further calcined samples at 300 and 500 °C. Though the calcination treatment diminishes the surface area of all systems, samples calcined at 500 °C still

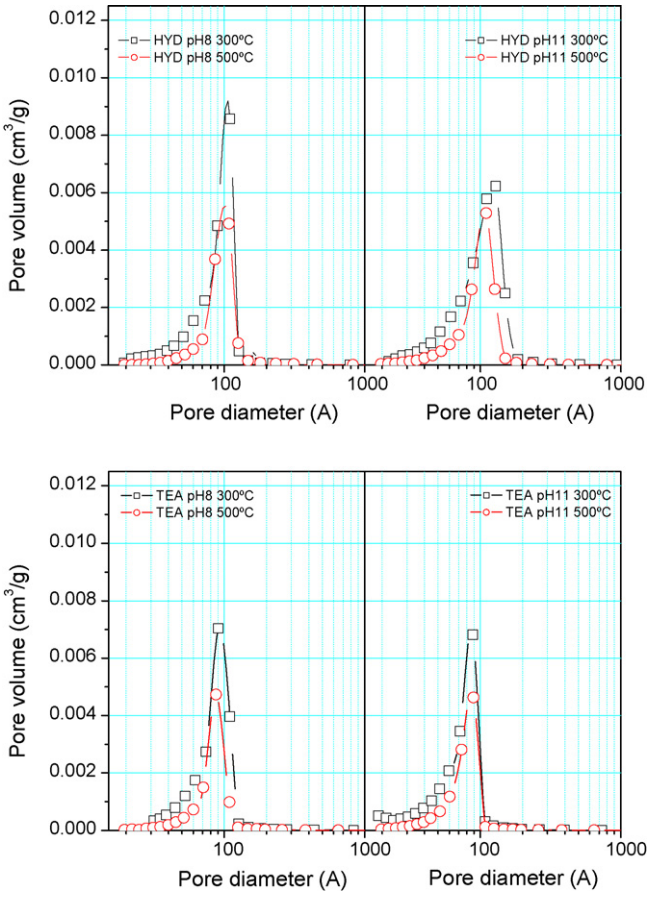

Fig. 4. Pore size distribution of hydrothermal and further calcined systems.

present relatively high surface area. Furthermore, hydrazine precipitated system still presents the same dependence between S_{BET} and pH, increasing the surface area as pH increases. On the contrary, for TEA precipitated one, the initial difference between the two pH samples seems to be reduced, being independent with pH precipitation value. It is also worthy to note that the hydrazine precipitated samples show higher surface area values with respect to TEA ones.

The pore size distribution depicted in Fig. 4 evidently denotes that calcination treatment at 300 and 500 °C do not lead to significant changes in the average pore diameter. Thus, for hydrazine precipitated TiO_2 post-calcination at 300 and 500 °C, the mean pore size is around 100–120 Å, while for TEA ones this value is somewhat lower (ca. 90 Å). Calcination treatment produces an homogeneous porous surface in all samples, independently of amine type or pH.

After calcination, no changes have been observed in the structural features of the systems. In all cases, the anatase phase is only present in XRD patterns. The further treatment at 300 and 500 °C only induces a notably improvement in the crystallinity of TiO_2, especially after calcination at 500 °C (Table 1). Thus, the mean crystallite size calculated from XRD peak broadening raises from ca. 9 nm for hydrothermal systems to ca. 18 nm calculated for samples calcined at 500 °C. There is no direct influence of the amine type or precipitating pH value upon the crystallite sizes.

Additionally and as expected, the morphology of calcined systems notably differs from hydrothermal ones. Calcination treatment clearly induces an important crystal growth and therefore leads to an improvement in the particles crystallinity. Fig. 5 shows the TEM images corresponding to hydrazine and TEA precipitated systems at pH 11 calcined at 500 °C. Homogeneous size and rather roundish in shape particles are found at each calcination temperature, exhibiting no aggregation in any case. The observed crystallite size are about 10–15 nm for systems calcined at 300 °C, and ca. 20 nm for samples calcined at 500 °C, according to the values calculated from XRD.

The band-gap calculated from the UV–vis diffuse reflectance spectra (not shown) corresponding to post-calcined samples at 300 and 500 °C are summarized in (Table 1). As it

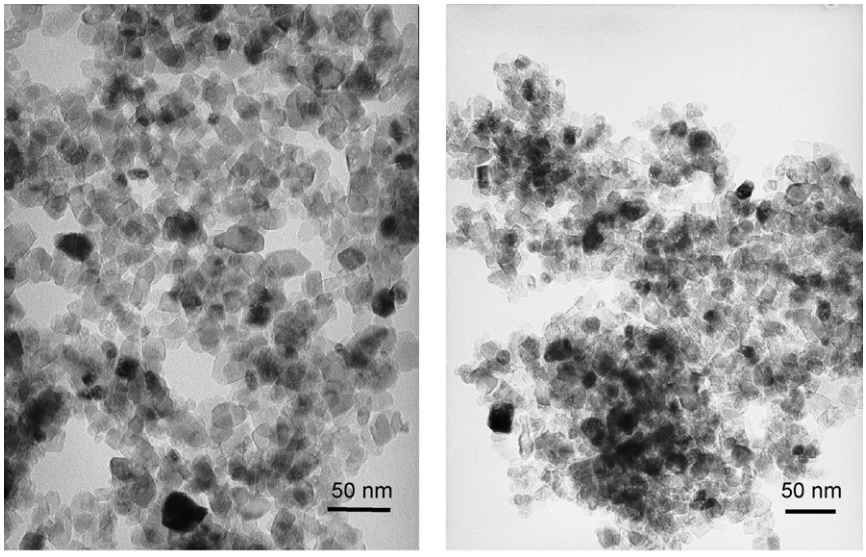

Fig. 5. TEM images of selected samples calcined at 500 °C: (a) TiO_2 HYD at pH 11 and (b) TiO_2 TEA at pH 11.

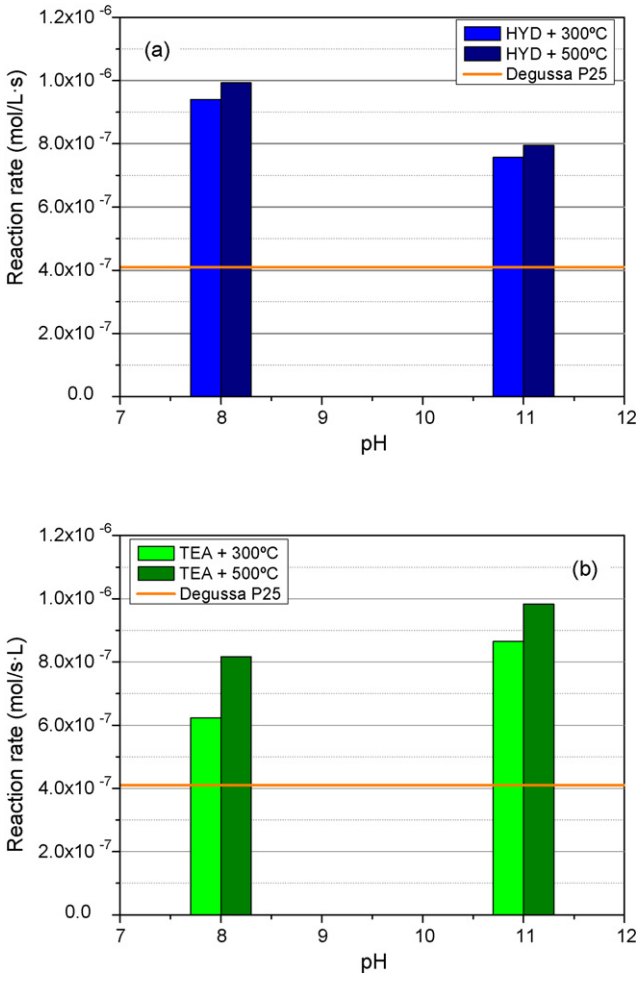

Fig. 6. Photocatalytic activity of hydrothermal and further calcined systems prepared from (a) HYD and (b) TEA.

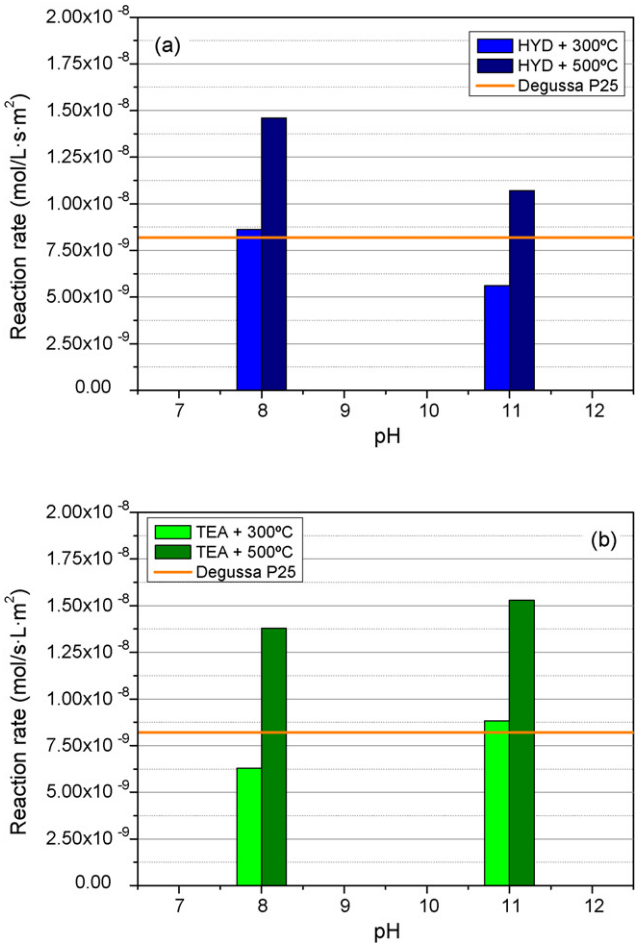

Fig. 7. Photocatalytic activity per surface area unit of hydrothermal and further calcined systems prepared from (a) HYD and (b) TEA.

can be seem, the band gap values are independent from the amine type used, the precipitation pH, as well as the calcination temperature, being in all cases 3.3 eV. This fact is related with the structural and morphology unmodification during calcination.

The photoactivities of calcined systems plainly show a significant enhancement with respect to uncalcined ones (Fig. 6). Moreover, the reaction rates are remarkably higher than that calculated for Degussa P25. Regarding to the hydrazine precipitated TiO_2, a further calcination treatment slightly differentiate both pH of precipitation. Thus, while hydrothermally treated systems display similar photoactivities, when calcined reaction rates slightly decrease as pH increases. In addition, it seems that the calcination temperature does not affect notably to the observed reaction rates, being similar for 300 and 500 °C. On the other hand, for samples obtained by precipitation with TEA it seems that there exists a certain effect in the calcination temperature. As a result, the calcination at 500 °C produces a significantly higher conversion rate than sample calcined at 300 °C. In the case of TEA system, it can be also observed the contrary dependence with pH than in the case of hydrazine one, keeping the same dependence as in the uncalcined series (Fig. 3a). Thus, in this system the conversion rates seem to increase as pH increases. From these results, we may infer that best photocatalytic activities are obtained by the system precipitated with hydrazine at pH 8 as well as system precipitated with TEA at pH 11, further calcined in both cases at 500 °C.

In order to elucidate the surface area contribution to the photoactivities of calcined systems we have represented the conversion rate per surface area unit (Fig. 7). It is worthy to note that by plotting the specific conversion rates systems calcined at 500 °C clearly raises up with respect to Degussa P25. Calcination at 300 °C is not sufficient for improving the structural situation and surface area still control the photoactivity. Thus, samples calcined at 500 °C plainly exhibit a good structural and surface situation, even better than Degussa P25. From these results, it is clear that the optimum precipitation pH is different for hydrazine and TEA, being 8 and 11, respectively.

4. Conclusions

We have studied the preparation of TiO_2 by different hydrothermal methods using hydrazine and TEA as precipitating agent. By varying the pH and performing an additional calcination treatment, we have optimised the photocatalytic

activity of our TiO_2 photocatalysts. The conversion rates for hydrothermally treated TiO_2 show similar values as for Degussa P25, especially at pH 8. Moreover, precipitation with hydrazine seems not to be influenced by the precipitation pH. In spite of the reasonable photoactivities observed, this behaviour is mainly due to the surface area contribution as denoted by the specific conversion rates plot. Calcination at 300 and 500 °C clearly enhances the photoactivities of hydrothermal TiO_2 systems. Therefore, hydrothermal treatment does not grant the finest performance in the catalyst for a photocatalytic application. This further calcination treatment would provide an optimal structural situation, reducing the number of defects or amorphous domains but keeping at the same time a relatively low crystallite size. As a result join surface and structural contributions lead to better photoactivity rates for phenol degradation. In this sense, calcination at 500 °C gives the best performance. At this temperature, relatively high surface area and well-crystallized anatase structure (non-aggregated and with homogeneous size and shape particles of about 18 nm) is obtained. The best photocatalytic conversion rates is achieved for TiO_2 prepared by precipitation with hydrazine at pH 8 and TEA at pH 11 post-calcined at 500 °C for 3 h.

Acknowledgements

Financial support (projects CTQ2004-05734-CO2-01 and CTQ2004-05734-CO2-02) and Junta de Andalucía (P.A.I. group references FQM181 and project P06-FQM-1406) are acknowledged. Ms. E. Pulido also wanted to thank her exchange fellowship within the FPI programme by the Spanish Ministerio de Educación y Ciencia.

References

[1] G. Colón, C. Belver, M. Fernández-García, in: M. Fernández-García, J.A. Rodríguez (Eds.), Synthesis, Properties and Application of Oxide Nanoparticles, Wiley, USA, 2007, , ISBN: 978-0-471-72405-6.
[2] O. Carp, C.L. Huisman, A. Reller, Prog. Solid State Chem. 32 (2004) 33.
[3] M. Tomkiewicz, Catal. Today 58 (2000) 115.
[4] C.C. Wang, Z. Zhang, J.Y. Ying, Nanostruct. Mater. 9 (1997) 583.
[5] Z. Zhung, C.C. Wang, R. Zakaria, J.Y. Ying, J. Phys. Chem. B 102 (1998) 10871.
[6] Yu.V. Kolen'ko, B.R. Churagulov, M. Kunst, L. Mazerolles, C. Colbeau-Justin, Appl. Catal. B: Environ. 54 (2004) 51.
[7] S. Boujday, F. Wünsch, P. Portes, J.F. Bocquet, C. Colbeau-Justin, Sol. Energy Mater. Sol. Cells 83 (2004) 421.
[8] K.M. Schindler, M. Kunst, J. Phys. Chem. 94 (1990) 8222.
[9] C. Colbeau-Justin, M. Kunst, D. Huguenin, J. Mater. Sci. 38 (2003) 2429.
[10] Y. Takahashi, Y. Oya, T. Ban, US Patent 6,770,216.
[11] Y.B. Ryu, S.S. Park, G.D. Lee, S.S. Hong, J. Ind. Eng. Chem. 12 (2006) 289.
[12] Y.B. Ryu, M.S. Lee, E.D. Jeong, H.G. Kim, W.Y. Jung, S.H. Baek, G.D. Lee, S.S. Park, S.S. Hong, Catal. Today 124 (2007) 88.
[13] I.M. Arabatzis, P. Faralas, Nano Lett. 3 (2003) 249.
[14] M.C. Hidalgo, M. Aguilar, M. Maicu, J.A. Navío, G. Colón, Catal. Today 129 (2007) 50.
[15] N. Serpone, D. Lawless, R. Khairutdinov, J. Phys. Chem. 99 (1995) 16646.
[16] J.C. Hong, C.V. Bang, D.H. Shin, H.S. Uhm, Chem. Phys. Lett. 413 (2005) 454.
[17] X. Chen, Y. Lou, A.C.S. Samia, C. Burda, L. Gole, Adv. Funct. Mater. 15 (2005) 41.
[18] K.M. Reddy, S.V. Manorama, A.R. Reddy, Mater. Chem. Phys. 78 (2002) 239.